pubs.acs.org/Biomac

Article

Effect of Moisture Content on Ion Diffusion and Glass Transition Temperature in Wood Cell Walls

Sina Youssefian, Mobin Vandadi, Joseph E. Jakes, and Nima Rahbar*

Cite This: *Biomacromolecules* 2024, 25, 666−674

Read Online

ACCESS | Metrics & More | Article Recommendations | Supporting Information

ABSTRACT: Understanding and controlling the diffusion of ions and chemicals within the secondary plant cell walls are pivotal in various applications of biomasses. Recent studies have shown that inorganic ion diffusion through secondary cell walls is controlled by a moisture-induced glass transition in amorphous polysaccharides, including amorphous cellulose and hemicelluloses. Understanding the diffusion of ions in these structures has been the subject of numerous recent experiments; however, a deep understanding of the underlying mechanisms of interactions between ion atoms and water/hemicellulose molecules is still lacking. This study uses molecular dynamics simulations to elucidate the diffusion mechanisms of potassium and chloride ions in the cell walls under varying moisture content. The results reveal that a higher moisture content leads to the formation of solvent layers around the ions and reduces the charge interaction between the functional groups of wood polymers and ions. Hence, a higher moisture content results in an improved diffusion rate of ions within the domain. The simulation results also show that higher moisture content lowers the glass transition temperature, promoting diffusion of ions in the system. In contrast, increases in the ion concentration increase the glass transition temperature of the system and degrade the diffusion of ions in the system.

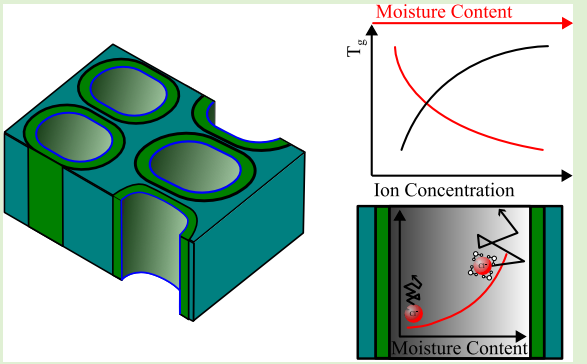

1. INTRODUCTION

Renewable lignocellulosic biomass is a valuable feedstock for biorefineries, which produce energy, chemicals, and fuels. Additionally, it continues to serve as the foundation for wood-based construction materials.[1−3] However, the complete utilization of lignocellulosic biomass is impeded by an incomplete understanding of various essential processes at the molecular scale. One such process is the diffusion of mineral ions through the cell walls of lignocellulosic materials.

The diffusion of mineral ions holds significance in several processes, including biomass pretreatments in biorefineries,[4] wood preservative treatments,[5] fungal decay of wood,[6−8] and corrosion of metal fasteners in wood.[9−11] Enhancing our understanding of the molecular mechanisms governing mineral ion diffusion is crucial for advancing research efforts to design the molecular architecture of lignocellulosic biomass for specific applications. For example, promoting diffusion could facilitate biomass breakdown into useful molecular components in biorefineries, while inhibiting diffusion could safeguard wood-based construction materials against degradation caused by decay and metal fastener corrosion.

Water plays a vital role in wood properties including cell wall diffusion.[12] All wood polymers have the capacity to absorb water, although the highly ordered cellulose chains within the cellulose fibrils exhibit lower water absorption in contrast to the more amorphous components that swell as a result of water absorption.[13] The moisture content (MC) of wood is defined as the water mass divided by the oven-dry mass of wood.[14] The MC of wood depends on the ambient temperature and relative humidity conditions. Below the fiber saturation point (FSP), which typically ranges from 30 to 40% MC depending on the definition used,[15] all water within the wood is bound within the cell walls. Above the FSP, additional water exists as free water within the larger cavities of the wood cells such as lumina and pits.

The first physical models for ion diffusion through the wood cell walls were developed based on the interpretation of the moisture-dependent electrical properties measured in wood, which spans 10 orders of magnitude depending on MC.[14] Much experimental evidence agrees that electrical conductivity in wood is ionic.[16−18] Therefore, the ion conductivity σ follows the usual relation

$$\sigma = \sum \mu_i n_i Z_i \tag{1}$$

where μ_i is the mobility of ion i, n_i is the concentration of ion i, and Z_i is the charge of ion i. In all of these early models, it was

Received: August 20, 2023
Revised: December 23, 2023
Accepted: December 26, 2023
Published: January 9, 2024

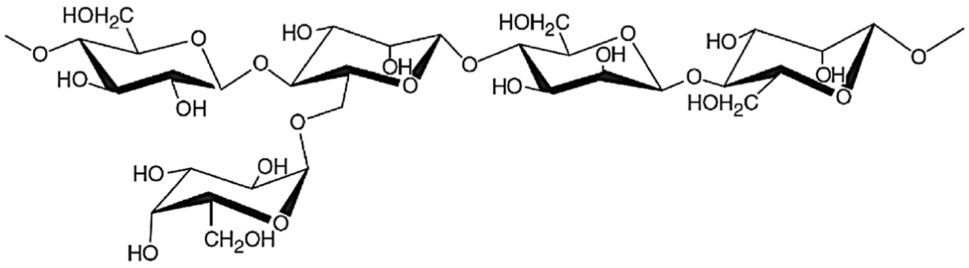

Figure 1. Principal structure of galactoglucomannans in softwood.

assumed that ionic conduction was an aqueous process occurring through pathways of free water or "loosely" bound water. Because the models are applied below the FSP, and therefore before free water forms in the wood cavities, they imply that these pathways exist inside the cell walls. The earliest model[19,20] proposed that ions conducted along water pathways that were disconnected, and μ_i depended on how long it took the ion to cross from one path to another. σ increased with increasing MC because μ_i increased as paths joined together, and there were fewer breaks. In 1963, Brown and co-workers[16] applied Hearle's model[21] to explain the moisture dependence of σ in wood. In Hearle's model, σ increases with MC because more ions become dissociated; thus, n_i increases and results in the increased σ. In 2008, Zelinka and co-workers[22] proposed a model based on percolation theory and asserted that pathways of loosely bound water reached a percolation threshold at 16% MC. Therefore, σ increased above the percolation threshold because μ_i increased at MC values higher than 16%. However, the water pathways that all of these early models assumed to exist inside of the cell wall have never been experimentally observed. Previous experimental observations of the loosely bound water in wood cell walls[22−24] are actually now understood to be an artifact of the sample preparation used in those studies.[25]

More recently, it was proposed and confirmed that mineral ion diffusion in secondary lignocellulosic cell walls occurs through interconnecting pathways of amorphous polysaccharides (amorphous cellulose and hemicelluloses) that have passed through their moisture-induced glass transition and are in their rubbery state.[26,27] This diffusion mechanism is a solid polymer diffusion mechanism that supplants previous models based on pathways of free water or loosely bound water inside wood cell walls. Therefore, polymer science should be used to understand diffusion through secondary wood cell walls.[12]

Molecular dynamics simulations provide a promising approach to further investigate the details of moisture-dependent ion diffusion in amorphous polysaccharides. In addition to studying rates of diffusion, the molecular relaxations and molecular-scale spatial distributions of water, hemicelluloses, and ions can also be studied as functions of MC by simulations. The glass transition temperature (T_g) of hemicelluloses, signifying the transition from a glassy to a rubbery state, is of particular interest because it is expected to significantly influence their properties. In hemicelluloses, variations in T_g have been shown to impact diffusion, moisture content, thermal stability, solubility, mechanical strength, and barrier properties.[16,21,28−34] Understanding these factors is critical for designing materials with tailored ion transport properties.

This study focuses on simulating the impact of moisture on the structure and diffusion behavior of potassium and chloride ions in the model amorphous polysaccharide galactoglucomannan, which is a hemicellulose commonly found in softwood from gymnosperm trees, such as conifers. These specific ions and polysaccharides were selected to facilitate a direct comparison between the simulation results and recent experimental measurements of ion diffusion through loblolly pine secondary cell walls.[35,36]

2. METHODS

In this study, galactoglucomannans were chosen because they are one of the primary hemicellulosic fractions of softwoods. They predominantly consist of hexoses, such as galactose, glucose, and mannose. The chemical composition analysis of pine, a representative softwood tree, also revealed that hexoses account for approximately 64% of its hemicellulose composition. Hence, the principal molecular structure of galactoglucomannans shown in Figure 1 was utilized to model the hemicelluloses present in pine.[37,38]

2.1. Moisture Content Simulations. Molecular dynamics simulations were performed using GROMACS software.[39] To simulate the behavior of hemicelluloses, six oligomers of galactoglucomannan, each composed of 25 repeating units, were assembled into periodic structures. These structures were created in seven configurations with varying amounts of water molecules, representing hemicelluloses with moisture contents (MC) of 0, 1, 2.5, 5, 10, 15, 20, or 25%. Additionally, two series of these hemicellulose structures were constructed, with 1 or 10 chloride and potassium ions incorporated into each structure. All of these atoms and molecules were packed in the simulation box using Packmol software[40] with a minimum distance of 2 Å between all atoms. Afterward, the structure was minimized using the conjugate gradient method. The Charmm-36 potential is used for this set of simulations,[41] and the SPC/E water model is used in these simulations.

Next, the assembled hemicellulose systems were subjected to a relaxation process using a series of NVT and NPT molecular dynamics simulations, each for 2 ns.[42] The relaxation process aimed to achieve equilibrium at 300 K without introducing artificial energy resulting from growing fragmented molecules in an empty box. Root-mean-square deviation (RMSD) was used to make sure that the system was completely relaxed. Following relaxation, structures with densities comparable to those of experimental data were selected for subsequent simulations. These selected structures represent periodic systems that realistically mimic the conformations of pine hemicellulose, with dimensions of approximately 5.5 × 5.5 × 5.5 nm^3.

NVE (constant number of particles, volume, and energy) dynamics simulations were conducted on the equilibrated models to investigate the Brownian motion of chloride and potassium ions within pine hemicellulose. The simulations were run for a duration of 2.5 ns, during which the ions moved according to the equations of motion.

To determine the diffusion coefficient (D) of the ions, the mean square displacement (MSD) was calculated relative to their initial positions. The MSD provides information about the average displacement of the ions over time. The diffusion coefficient can be obtained from the slope of the MSD plot. The calculation of the diffusion coefficient using the MSD is performed as follows:

https://doi.org/10.1021/acs.biomac.3c00857
Biomacromolecules 2024, 25, 666−674

$$D = \frac{1}{6}\lim_{t\to\infty}\frac{\mathrm{d(MSD)}}{\mathrm{d}t}$$

where MSD is given by

$$\mathrm{MSD} = \frac{1}{N}\sum_{i=1}^{N}\langle |r_i(t) - r_i(0)|^2\rangle$$

where N is the number of ions, and $r_i(t)$ and $r_i(0)$ are the current and initial position vectors of ith ions, respectively. Hence, the rate of MSD variation with time can be used to evaluate the self-diffusion coefficient of chloride and potassium ions undergoing random Brownian motion in three dimensions.

2.2. Glass Transition Temperature Simulations. Another set of simulations was performed to investigate the glass transition temperature of the galactoglucomannans. In these simulations, systems consisting of 25 repeating units of the hemicellulose were created and replicated to represent different moisture contents, ranging from 0 to 25%. Additionally, three sets of simulations were performed, one with 0 ions, one with 1 ion pair, and the last with 10 ion pairs. Similar to the previous set, the hemicelluloses, water molecules, and ion atoms were packed inside the simulation box (with a similar size to the previous set) using Packmol. Then, the energy of the system was minimized by using the conjugate gradient method to remove any possible energy jumps in the system. The water model in this set was similar to the previous set of simulations and the Charmm-36 potential was used for interatomic interactions.[41]

Afterward, each system was equilibrated using the Noose−Hoover ensemble for a duration of 2.5 ns. This ensemble allowed the system to reach a stable state at a temperature of 270 K. Following the equilibration, the temperature of the system was gradually increased from 270 to 420 K, with increments of 10 K. Each increment was performed linearly over a period of 1 ns, during which the temperature was held constant for an additional 1 ns to ensure thermal equilibrium.

Throughout the constant temperature simulations, the root-mean-square deviation of the system was continuously monitored to ensure that the system reached stability by the end of the 1 ns period. This verification step was crucial in confirming that the system achieved a consistent and reliable state for subsequent analysis.

The system's density was calculated at each temperature step to examine its evolution as a function of temperature and moisture content. By observation of the changes in density, particularly in relation to the glass transition temperature, valuable insights were gained regarding the structural transformations and the effects of moisture on the hemicellulose material.

These simulations aimed to capture the behavior of galactoglucomannans across a range of temperatures and moisture contents, ultimately providing valuable data to determine the glass transition temperature and better understand the dynamics and properties of the hemicellulose material under different conditions.

3. RESULTS AND DISCUSSION

Figure 2 illustrates the relationship between the density and moisture content (MC) for hemicelluloses containing different numbers of chloride and potassium ions. The findings indicate that the density of the pine hemicellulose galactoglucomannan decreases as MC increases, irrespective of the number of ions present. However, the rates at which the density changes are not the same. Hemicellulose with more ions experienced a more pronounced decrease in density as MC increased. At MC values below 15%, the hemicellulose containing more ions exhibits a higher density than the models with fewer ions. However, all three models exhibited nearly similar densities at higher MC levels.

Figure 3 illustrates the variation of diffusion coefficients with moisture content (MC) for chloride and potassium ions in the 1-ion pair system. The MSD plots used to calculate the

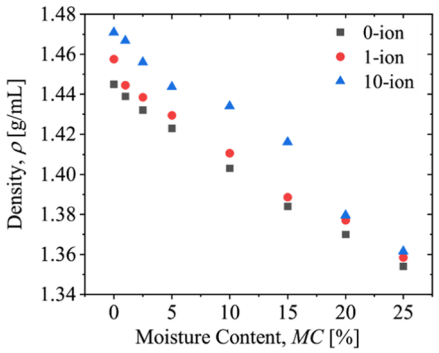

Figure 2. Density vs moisture content for hemicelluloses with 0, 1, and 10 chloride and potassium ion pairs at 300 K.

diffusion constants are shown in the Supporting Information. The diffusion coefficients for the 10-ion pairs system had the same trends with MC but the values were on average 12% lower. In both systems, the diffusion coefficients increased exponentially as the MC increases. While the trend of diffusion coefficient growth is consistent for both ions, there was a distinct difference in the growth rates, particularly at higher MC levels. Chloride diffusion coefficients (Figure 3a) increased from 2.22×10^{-9} to 3.71×10^{-6} cm^2/s. On the other hand, the diffusion coefficients of potassium (Figure 3b) increased from 4.69×10^{-9} to 9.02×10^{-7} cm^2/s. Below 15% MC, potassium and chloride diffusion rates were within the same order of magnitude. However, above 15%, the diffusion coefficient of chloride became approximately 1 order of magnitude higher than that of potassium. This difference was consistent with the previous studies,[43] which reported that anions diffuse faster than cations. Sarker et al. explained that partial negative charges of functional groups in the wood polymers (carboxylates) attract the cations in the system and slow their movement, while anions are repelled by these groups and diffuse in the wood cells much easier.

Figure 4 presents the experimental diffusion coefficients of potassium ion (K^+) and chloride (Cl^-) that were experimentally measured in the S2 secondary wood cell wall of loblolly pine[36] and compares them with the results obtained from the molecular dynamics (10-ion pair system) simulations performed in this study. In the experimental setup, ion gradients were created in the cell wall layer by applying a small drop of KCl aqueous solution to a 2 μm thick wood section. The wood section was then conditioned at different relative humidity levels, namely, 70, 75, or 80%. Time-lapse images of ion diffusion through the cell wall were captured using synchrotron-based X-ray fluorescence microscopy (XFM). The diffusion constants for K and Cl were calculated by analyzing the time-dependent concentration gradients. This analysis assumed that the diffusion followed Fick's second law for nonsteady state diffusion and that the diffusion coefficient remained constant.

Notably, the experimental diffusion constants are 2−3 orders of magnitude lower than those obtained from the MD simulations. However, both the experimental and simulated diffusion coefficients exhibited a similar increase pattern with MC, which suggested that diffusion in the simulations and experiments was controlled by similar phenomena. There are numerous factors that likely contribute to the discrepancy in the diffusion constant values. A major factor is that the simulations and experiments measured two different types of

https://doi.org/10.1021/acs.biomac.3c00857
Biomacromolecules 2024, 25, 666−674

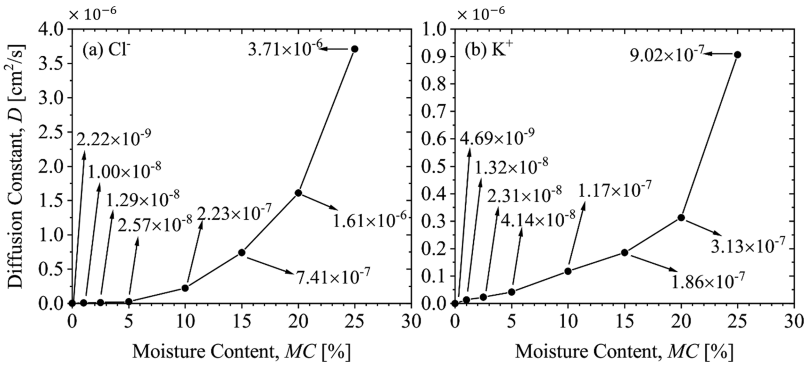

Figure 3. Diffusion rate of (a) chloride and (b) potassium ions vs moisture content from the 1-ion pair system at 300 K.

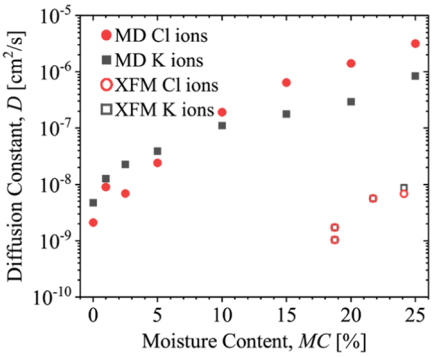

Figure 4. K^+ and Cl^- diffusion constants measured using molecular dynamics (MD) and experimental measurements in loblolly pine (*Pinus taeda*) S2 secondary cell wall layers using X-ray fluorescence microscopy (XFM).[26] The moisture contents for the XFM measurements were calculated using relative humidity during the experiment and the hemicellulose isotherm of Cousins' work.[44]

diffusion. In the experiments, diffusion occurred at a concentration gradient in which ions moved from volumes of higher concentration to lower concentrations. To maintain charge neutrality, both cations and anions were required to diffuse together. For example, Jakes et al.[36] measured the diffusion of ions deposited by KCl or $CuCl_2$ aqueous salt solutions. The chloride diffusion rates depended on the cation with chloride in the $CuCl_2$ experiment diffusing about an order of magnitude slower than the chloride in the KCl experiment. The copper ion and two chlorides diffused more slowly because they were effectively a larger diffusant than the potassium ion and single chloride that had to diffuse together in the KCl experiment. In the current simulations, self-diffusion was assessed in which an individual ion moved without having to have another ion move with it to maintain charge neutrality. Without the constraint of having to have multiple ions move together to maintain charge neutrality, the ions in the simulations diffused faster.

Other possible factors for the discrepancy in diffusion constant values include the type of amorphous polysaccharide tested, shapes of the hemicellulose volumes, hydrostatic pressures inside of swelling wood cell walls, and differences in ion concentrations. Galactoglucomannan is only one type of amorphous polysaccharide inside loblolly pine cell walls. Amorphous cellulose and other types of hemicelluloses such as arabinoglucuronoxylan are also present and likely influenced the experimentally measured diffusion coefficients. The hemicellulose domains within the cell wall also have different shapes and configurations compared with the 5.5 nm cubic model used in the simulations. Inside the cell wall, hemicelluloses are likely elongated cylinders with diameters ranging from 1 to 3 nm. Diffusion predominantly occurs along the length of these cylinders, making the system different from the MD model. Additionally, experimental studies show that the hydrostatic pressure in the water-swollen cell wall can be as high as 100 MPa.[45] This pressure could also reduce the available free volume, impeding diffusion. Finally, increases in ion concentrations decrease diffusion coefficients, as observed in the comparison between the simulated one-ion pair and 10-ion pair systems. Concentrations of ions in the experiments are in order of 1000 mol/m^3, while in the 5.5^3 nm^3 simulation size, the 1−10 ion would result in a concentration of 9.98−99.81 mol/m^3. This higher concentration of ions would likely result in the clustering of ions in the system.

To gain valuable insights into the spatial arrangement of atoms within the hemicellulose, we used the radial distribution function (RDF), denoted as $g(r)$. Figure 5 illustrates the RDF

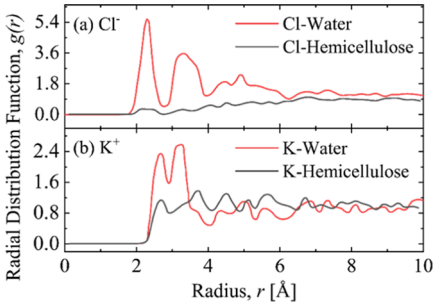

Figure 5. Radial distribution function of (a) chloride and (b) potassium with water molecules (red line) and hemicellulose (black line) at 25% MC.

comparisons between ions (potassium and chloride) and water molecules as well as between ions and hemicellulose chains at the 25% moisture content (MC). In both cases, the RDFs between ions and water molecules exhibited higher peak values compared to the RDF between ions and hemicellulose chains. This observation indicated that water molecules surrounded the ions, decreasing the interactions between the ions and hemicellulose chains. Figure 5a displays the RDF for chloride ions, revealing the accumulation of three layers of water molecules around the ions. These layers are located at distances of 2.2, 3.3, and 4.4 Å. The intensity of water molecules surrounding the chloride ions is notably high, resulting in minimal interaction between the chloride ions and hemicellulose chains. In Figure 5b, the RDF for potassium ions

https://doi.org/10.1021/acs.biomac.3c00857
Biomacromolecules 2024, 25, 666−674

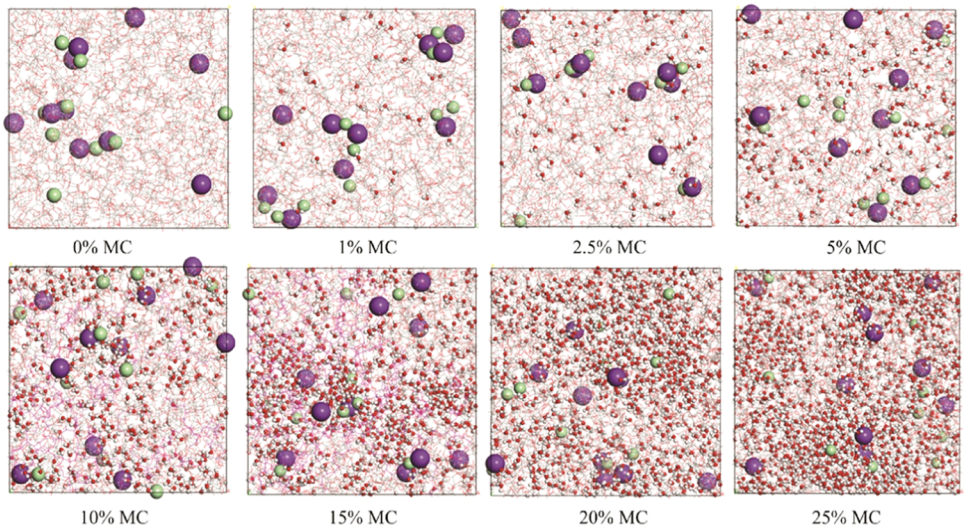

Figure 6. Ion and water molecule distributions in relaxed pine hemicellulose. The purple spheres represent chloride atoms, the green spheres represent potassium atoms, and the remaining entities (red atoms connected to white atoms) denote water molecules. At lower moisture content, the ions conglomerate. However, as the moisture content increases, layers of water are formed around the ions.

shows the presence of two layers of water molecules located at distances of 2.7 and 3.3 Å surrounding the ions. The hemicellulose chains do not exhibit significant alignment or interaction with the potassium ions. These findings demonstrated that water molecules play a crucial role in surrounding and solvating the ions, thereby reducing their interactions with the hemicellulose chains in the system.

The predicted behavior by RDF plots can also be visually seen in Figure 6. This figure shows that increases in the MC of the system resulted in hydration shells around the ions in the system. However, in the low MC systems, the ions have direct interactions with the hemicellulose.

Figure 7 displays the RDF between potassium and chloride ions at different MCs. The RDF diagram for each MC

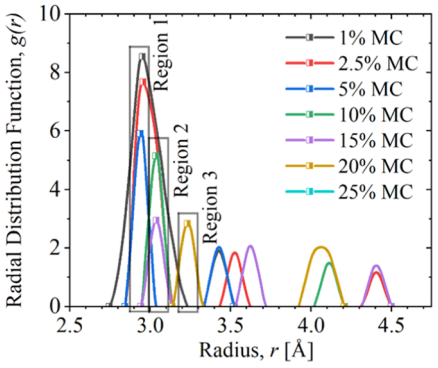

Figure 7. Radial distribution function between potassium and chloride. For 1, 2.5, and 5% moisture content (MC), the closest distance between potassium and chloride atoms is around 2.95 Å. For 10% and 15% MC, at 3.1 Å and for 20%, at 3.25 Å. For the case of 25%, no peak is observed up to 5 Å.

exhibited a prominent peak at the beginning, followed by successive shorter peaks. The RDFs can be divided into three regions. The first region, observed at 2.95 Å, corresponds to the potassium-chloride distance at 1, 2.5, and 5% MC. In this region, the intensity of the peaks gradually decreases as the MC increases. The second region, occurring at 3.1 Å, represents the potassium-chloride distance for 10 and 15% MC. The intensity of the peak is higher for 10% MC compared to 15% MC. The third region, characterized by a short peak at 3.25 Å, corresponds to the potassium-chloride distance at 20% MC. These results indicated that as water molecules permeate the pine hemicellulose structure, they accumulate around chloride and potassium ions, thereby interfering with their interactions. This accumulation of water molecules increases the distance between the ions and prevents the formation of ion clusters at higher MCs.

As shown in both Figures 6 and 7, at low MC, we observed that chloride and potassium ions tend to come together and form clusters. Due to their larger sizes, this clustering contributed to slower migration rates. However, at high MC, the presence of water molecules disrupted the formation of these clusters. The polar water molecules were strongly attracted to ions through electrostatic forces, which caused the ion clusters to dissolve. As a result, layers of water molecules are formed around the chloride and potassium ions instead of cluster formations. The water molecules acted as carriers for the ions within the pine hemicellulose structure, which promoted diffusion.

Overall, these results suggest that increasing the MC dissociates ion clusters to individual chloride and potassium ions. Since individual ions are smaller than clusters, they experience less hindrance from surrounding molecules and can diffuse more freely. Additionally, the hydration shells facilitate ion movement through the hemicellulose structure. This observation supports the physics behind Brown and co-workers'[16] application of Hearle's model[21] in which they assert ionic conductivity experimentally increases with MC because more ions dissociate at higher MC. However, although ion dissociation likely plays an important role, it is not expected to fully explain the MC dependence of ionic conductivity in wood. It is also known that the amorphous polysaccharides' glass transition temperature (T_g) has a primary role in controlling ionic diffusion.[12,26]

The T_g of the hemicellulose was studied here by analyzing density changes as a function of the temperature, MC, and ion concentration. Figure 8 illustrates the measured temperature-dependent density for 0-ion, 1-ion, and 10-ion pair systems

https://doi.org/10.1021/acs.biomac.3c00857
Biomacromolecules 2024, 25, 666−674

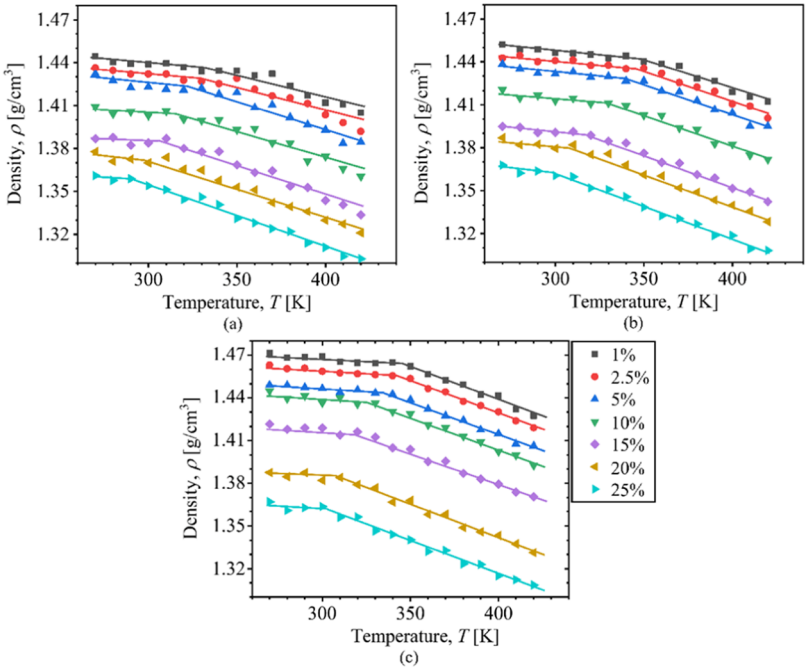

Figure 8. Density of the system as a function of the temperature in the (a) 0 ion, (b) 1 ion pair, and (c) 10 ion pair systems. The bilinear fit shows the glass transition temperature in the system.

with increasing MC. The 0- and 1-ion pair systems had similar densities. The 10-ion pair system had substantially higher density, especially at 15% MC and below. The difference in the density behavior for the 10-ion pair system can be attributed to the formation of solvation shells around the ions in the presence of water molecules. In systems containing ions, the surrounding water molecules arrange themselves in distinct solvation shells, altering the water behavior compared with systems without ions and resulting in a tighter packing of water molecules in the system. This increases the density of the system. In the case of the 1- ion pair system, the presence of a single ion pair is not substantial enough to significantly influence the system's overall behavior. Consequently, the change in density behavior is only modest, with a slight alteration in the rate of density change with MC. On the other hand, the ions in the 10-ion pair system had a more substantial impact on the overall density of the system.

Subsequently, T_g was determined by analyzing density changes as a function of temperature. The T_g was determined at the temperature where the density rate changes, which is found at the intersection of the two lines plotted for each data set in Figure 8. The lines in Figure 8 were plotted after minimizing the residual sum of squares from the first and second fits. The calculated T_g's are shown in Figure 9. This plot clearly shows the pattern of T_g with respect to the ion concentration and moisture content in the system. The T_g progressively decreased as the MC increased, irrespective of the ion concentration. However, for a given MC, the T_g increased with increasing number of ions. The dependence of T_g with MC and ion concentrations indicated that MC and ion concentration both influence the system's behavior, particularly in relation to its structural dynamics. The presence of additional plasticizing water molecules in the system introduces greater molecular mobility and disrupts the intermolecular interactions, thereby facilitating changes in the structural arrangements of the hemicellulose chains that promote diffusion. In contrast, increased ion concentrations increased T_g, which likely means decreased molecular mobility and hindered diffusion.

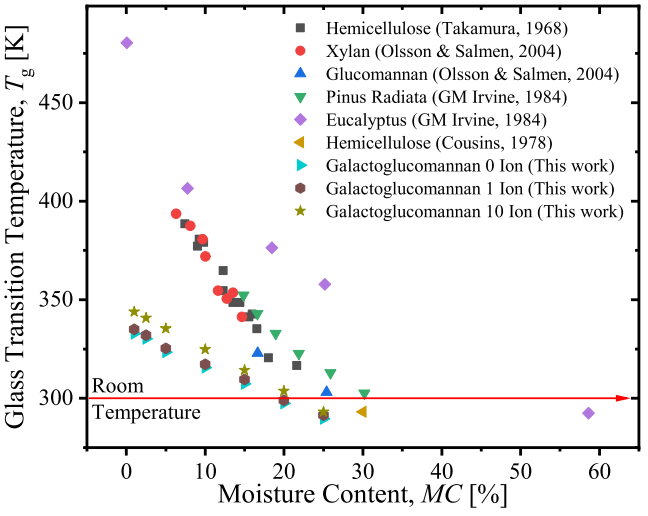

Figure 9. Extracted hemicelluloses' glass transition temperatures (T_g) as a function of the moisture content (MC) from experimental values in the literature and from the molecular dynamic (MD) simulations in this work. Experimental results include hemicelluloses extracted from *Pinus densiflora*,[46] hemicelluloses extracted from *Pinus radiata*,[47] hemicelluloses extracted from *Eucalyptus regnans*,[47] hemicelluloses extracted from *P. radiata*,[48] xylan from birch,[49] and glucomannan from *Amorphophallus Konjac*.[49] From the MD simulations, the T_g for the 10-ion pair system drops below 300 K when it reaches 20% MC. However, for the 1-ion system, the T_g drops below 300 K when it reaches 25% MC.

Additionally, Figure 9 includes experimental T_g values from the literature as a function of MC for the extracted hemicelluloses. The overall predicted T_g values from the molecular dynamics simulations are lower than the reported

https://doi.org/10.1021/acs.biomac.3c00857
Biomacromolecules 2024, 25, 666−674

experimental values. At room temperature, most of the experimental T_g values are at about 5−10% higher MC. This difference likely arises from the different types of measurements that were used to determine T_g and differences in molecular structures between studies. However, there is overall consistency between the simulations and experiments, as all of the T_g's decrease with respect to the MC and many of the rates of decreases are similar.

A notable difference between the experimental and numerical results is the onset of observed ionic diffusion. In experimental XFM studies of potassium and chloride ion diffusion through wood cell walls, the onset relative humidity (RH) threshold for which ion diffusion could be observed was in the range of 60−67% RH.[35] Using the hemicellulose sorption isotherm of Cousins,[44] 60−67% RH corresponds to about 17−20% MC for hemicelluloses. In the molecular dynamics simulations, ionic diffusion can be observed and measured at all MC including 0% MC. This difference in observable behavior between experiments and simulations can be addressed by considering how far the ions moved in the simulations. The movement of atoms at a specific diffusion rate is calculated using the equation $\chi = \sqrt{2Dt}$, where χ represents the distance traveled, D is the diffusion coefficient, and t is time. By applying this equation to the diffusion rates obtained from 2 ns molecular dynamics simulations, it becomes evident that ions only move approximately 0.03 nm at the lowest MC. Considering that the length of a xylan monomer is approximately 0.9 nm, it can be concluded that at low MC, ions are confined within molecular-scale holes and do not significantly move to different locations within the polymeric structure. However, the diffusion coefficients in Figure 3 at 20% and higher MC correlate to diffusion distances that exceed the monomer lengths of the polymer structure, indicating that ions are now diffusing to different locations along a polymer chain. It makes physical sense that ionic diffusion can only be observed experimentally by XFM when ions are able to move longer distances, like 1 nm or more, to different locations in the polymer structure. These results indicate that conditions in which simulated diffusion distances exceed the monomer length should correspond to when diffusion can be effectively observed experimentally.

This transition from confined diffusion at low MC to more extensive diffusion at higher MC and the onset of diffusion that can be detected experimentally with XFM[35,36] occurs when hemicelluloses are at about 20% MC. This MC agrees well with the simulation results for T_g. The T_g results fell below room temperature (300 K) between 20 and 25% MC depending on ion concentration (Figure 9). Although the experimental T_g's of extracted hemicelluloses in Figure 9 mostly fall below room temperature in the higher 25−30% MC range, the values from the extracted hemicelluloses may not correspond to the T_g of the in situ amorphous polysaccharides in the intact cell wall. Diffusion observed by XFM corresponds to this in situ T_g. For instance, Jakes et al.[26] reviewed literature T_g for both extracted and in situ hemicelluloses and found that the T_g's of in situ hemicelluloses were often reported at lower relative humidity values than extracted hemicelluloses. Overall, relations between diffusion and T_g are consistent with the current understanding that mineral ion diffusion in wood cell walls occurs through interconnecting pathways of rubbery amorphous polysaccharides (amorphous cellulose and hemicelluloses) that are below their T_g and in their rubbery state.[12,26]

4. CONCLUSIONS

The focus of this study was to investigate the impact of the moisture content and ion concentration on the diffusion coefficient of ions and glass transition temperature within hemicelluloses in wood cell walls. We used molecular dynamics simulations to examine the behavior of ions and water molecules in the presence of hemicellulose molecules.

Our findings are summarized below:

- The glass transition temperature shows a negative correlation with increasing moisture content and a positive correlation with rising ion concentration within the system.
- When the diffusion coefficient in a cell wall is large enough that ions can travel distances longer than the length of a monomer, the ion diffusion will be observable experimentally.
- Solvation shells are formed around the ions as the moisture content increases. These solvents' shells surround and interact with the ions, facilitating their movement within the system. This phenomenon leads to enhanced diffusion of ions in the wood cell walls.
- The diffusion rate of chloride ions outperforms that of potassium ions at higher moisture content. This can be attributed to the number of solvation layers surrounding each ion where potassium ions exhibit two layers of solvent around them, while chloride ions exhibit three layers. The partial negative charges of functional groups in the wood polymers (carboxylates) also likely attracted the cations in the system and slowed their movement.

By establishing the relationship among moisture content, ion concentration, glass transition temperature, and ion diffusion, this study sheds light on the intricate interplay of these factors in determining the dynamic behavior of hemicellulose systems. The findings highlight the importance of considering moisture and ion effects in designing materials with desired diffusion properties for various applications, such as energy storage, drug delivery, and ion-conductive membranes.

■ ASSOCIATED CONTENT

Supporting Information

The Supporting Information is available free of charge at https://pubs.acs.org/doi/10.1021/acs.biomac.3c00857.

Raw mean square displacement data from the molecular dynamic simulations used to calculate the diffusion rate of the ions in the hemicellulose; at lower moisture contents, the MSD of the ions are at the range of self-diffusion and the lines cannot be distinguished; for that, log−log plot is used to make the lines clear (PDF)

■ AUTHOR INFORMATION

Corresponding Author

Nima Rahbar − *Department of Civil, Environmental and Architectural Engineering, Worcester Polytechnic Institute, Worcester, Massachusetts 01609, United States; Department of Mechanical Engineering, Worcester Polytechnic Institute, Worcester, Massachusetts 01609, United States;* orcid.org/0000-0003-0159-0025; Email: nrahbar@wpi.edu

Authors

Sina Youssefian − *Department of Civil, Environmental and Architectural Engineering, Worcester Polytechnic Institute,*

https://doi.org/10.1021/acs.biomac.3c00857
Biomacromolecules 2024, 25, 666−674

Worcester, Massachusetts 01609, United States; Advanced Semiconductor Materials Lithography (ASML), Wilton, Connecticut 06897, United States

Mobin Vandadi − *Department of Civil, Environmental and Architectural Engineering, Worcester Polytechnic Institute, Worcester, Massachusetts 01609, United States;* orcid.org/0000-0003-4785-9675

Joseph E. Jakes − *Forest Biopolymers Science and Engineering, USDA Forest Service, Forest Products Laboratory, Madison, Wisconsin 53726, United States*

Complete contact information is available at: https://pubs.acs.org/10.1021/acs.biomac.3c00857

Notes

The authors declare no competing financial interest.

REFERENCES

(1) Bergman, R.; Puettmann, M.; Taylor, A.; Skog, K. E. The Carbon Impacts of Wood Products. *For. Prod. J.* **2014**, *64* (7−8), 220−231.

(2) Jakes, J. E.; Arzola, X.; Bergman, R. N.; Ciesielski, P. N.; Hunt, C. H.; Rahbar, N.; Tshabalala, M. A.; Wiedenhoeft, A. C.; Zelinka, S. L. Not Just Lumber—Using Wood in the Sustainable Future of Materials, Chemicals, and Fuels. *JOM* **2016**, *68* (9), 2395−2404.

(3) Ragauskas, A. J.; Williams, C. K.; Davison, B. H.; Britovsek, G.; Cairney, J.; Eckert, C. A.; Frederick, W. J.; Hallett, J. P.; Leak, D. J.; Liotta, C. L.; Mielenz, J. R.; Murphy, R.; Templer, R.; Tschaplinski, T. The Path Forward for Biofuels and Biomaterials. *Science* **2006**, *311* (5760), 484−489.

(4) Wei, H.; Donohoe, B. S.; Vinzant, T. B.; Ciesielski, P. N.; Wang, W.; Gedvilas, L. M.; Zeng, Y.; Johnson, D. K.; Ding, S.-Y.; Himmel, M. E.; Tucker, M. P. Elucidating the Role of Ferrous Ion Cocatalyst in Enhancing Dilute Acid Pretreatment of Lignocellulosic Biomass. *Biotechnol. Biofuels* **2011**, *4* (1), 48.

(5) Lebow, S. T. Wood Preservation. In *Wood Handbook: Wood as an Engineering Material*, General Technical Report FPL-GTR-190; Forest Products Laboratory: Madison, WI, 2010; pp 15.1−15.28.

(6) Arantes, V.; Jellison, J.; Goodell, B. Peculiarities of Brown-Rot Fungi and Biochemical Fenton Reaction with Regard to Their Potential as a Model for Bioprocessing Biomass. *Appl. Microbiol. Biotechnol.* **2012**, *94* (2), 323−338.

(7) Goodell, B.; Jellison, J.; Liu, J. B.; Daniel, G.; Paszczynski, A.; Fekete, F. A.; Krishnamurthy, S. S.; Jun, L.; Xu, G. Low Molecular Weight Chelators and Phenolic Compounds Isolated from Wood Decay Fungi and Their Role in the Fungal Biodegradation of Wood1This Is Paper 2084 of the Maine Agricultural and Forest Experiment Station.1. *J. Biotechnol.* **1997**, *53* (2−3), 133−162, DOI: 10.1016/s0168-1656(97)01681-7.

(8) Ringman, R.; Pilgård, A.; Brischke, C.; Richter, K. Mode of Action of Brown Rot Decay Resistance in Modified Wood: A Review. *Holzforschung* **2014**, *68* (2), 239−246, DOI: 10.1515/hf-2013-0057.

(9) Baker, A. J. Corrosion of Metals in Preservative - Treated Wood. In *Wood Protection Techniques and the Use of Treated Wood in Construction*; Forest Products Laboratory: Madison, USA, 1988; pp 99−101.

(10) Zelinka, S. L. Corrosion of Metals in Wood Products. In *Developments in Corrosion Protection*; Intech: Hongkong, 2014; pp 567−592.

(11) Zelinka, S. L.; Stone, D. S. Corrosion of Metals in Wood: Comparing the Results of a Rapid Test Method with Long-Term Exposure Tests across Six Wood Treatments. *Corros. Sci.* **2011**, *53* (5), 1708−1714.

(12) Jakes, J. E.; Hunt, C. G.; Zelinka, S. L.; Ciesielski, P. N.; Plaza, N. Z. Effects of Moisture on Diffusion in Unmodified Wood Cell Walls: A Phenomenological Polymer Science Approach. *Forests* **2019**, *10* (12), 1084.

(13) Hofstetter, K.; Hinterstoisser, B.; Salmén, L. Moisture Uptake in Native Cellulose: The Roles of Different Hydrogen Bonds: A Dynamic FT-IR Study Using Deuterium Exchange. *Cellulose* **2006**, *13* (2), 131−145.

(14) Glass, S.; Zelinka, S. Moisture Relations and Physical Properties of Wood. In *Wood handbook: Wood as an Engineering Material*; Forest Products Laboratory: Madison, 2021; pp 1−19.

(15) Zelinka, S. L.; Glass, S. V.; Jakes, J. E.; Stone, D. S. A Solution Thermodynamics Definition of the Fiber Saturation Point and the Derivation of a Wood−Water Phase (State) Diagram. *Wood Sci. Technol.* **2016**, *50* (3), 443−462.

(16) Brown, J. H.; Davidson, R. W.; Skaar, C.; Skaar, C. Mechanism of Electrical Conduction in Wood. *For. Prod. J.* **1963**, *13* (10), 455−459.

(17) Clark, J. D.; Williams, J. W. The Electrical Conductivity of Commercial Dielectrics and Its Variation with Temperature. *J. Phys. Chem. A* **1933**, *37* (1), 119−131.

(18) Langwig, J. E.; Meyer, J. A. Ion Migration in Wood Verified by Neutron Activation Analysis. *Wood Sci.* **1973**, *6* (1), 39−50.

(19) Murphy, E. J.; Walker, A. C. Electrical Conduction in Textiles. I the Dependence of the Resistivity* of Cotton, Silk and Wool on Relative Humidity and Moisture Content. *J. Phys. Chem. A* **1928**, *32* (12), 1761−1786.

(20) O'Sullivan, J. B. 31—THE CONDUCTION of ELECTRICITY through CELLULOSE: Part v. the EFFECT of TEMPERATURE. *J. Text. Inst. Trans.* **1948**, *39* (11), T368−T384.

(21) Hearle, J. W. S. The Electrical Resistance of Textile Materials: IV. Theory. *J. Text. Inst. Trans.* **1953**, *44* (4), T177−T198.

(22) Zelinka, S. L.; Glass, S. V.; Stone, D. S. A Percolation Model for Electrical Conduction in Wood with Implications for Wood-Water Relations. *Wood Fiber Sci.* **2008**, *40* (4), 544−552.

(23) Nakamura, K.; Hatakeyama, T.; Hatakeyama, H. Studies on Bound Water of Cellulose by Differential Scanning Calorimetry. *Text. Res. J.* **1981**, *51* (9), 607−613.

(24) Thygesen, L. G.; Elder, T. Moisture in Untreated, Acetylated, and Furfurylated Norway Spruce Monitored during Drying below Fiber Saturation Using Time Domain NMR. *Wood Fiber Sci.* **2009**, *41* (2), 194−200.

(25) Zelinka, S. L.; Lambrecht, M. J.; Glass, S. V.; Wiedenhoeft, A. C.; Yelle, D. J. Examination of Water Phase Transitions in Loblolly Pine and Cell Wall Components by Differential Scanning Calorimetry. *Thermochim. Acta* **2012**, *533* (1), 39−45.

(26) Jakes, J. E. Mechanism for Diffusion through Secondary Cell Walls in Lignocellulosic Biomass. *J. Phys. Chem. B* **2019**, *123* (19), 4333−4339.

(27) Jakes, J. E.; Plaza, N. Z.; Stone, D. S.; Hunt, C. G.; Glass, S. V.; Zelinka, S. L. Mechanism of Transport through Wood Cell Wall Polymers. *J. For. Prod. Ind.* **2013**, *2* (6), 10−13.

(28) Chu, J.; Wang, W.; Feng, J.; Lao, C.; Xi, K.; Xing, Lü.; Han, K.; Li, Q.; Song, L.; Li, P.; Li, X.; Bao, Y. Deeply Nesting Zinc Sulfide Dendrites in Tertiary Hierarchical Structure for Potassium Ion Batteries: Enhanced Conductivity from Interior to Exterior. *ACS Nano* **2019**, *13* (6), 6906−6916.

(29) Drake, A. C.; Lee, Y.; Burgess, E. M.; Karlsson, J. O. M.; Eroglu, A.; Higgins, A. Z. Effect of Water Content on the Glass Transition Temperature of Mixtures of Sugars, Polymers, and Penetrating Cryoprotectants in Physiological Buffer. *PLoS One* **2018**, *13* (1), No. e0190713.

(30) Guo, Y.; Zhang, Z.; Dou, J.; Liu, G.; Li, X.; Zhao, J. Structural Characterization of Corn Fiber Hemicelluloses Extracted by Organic Solvent and Screening of Degradation Enzymes. *Carbohydr. Polym.* **2023**, *313*, 120820.

(31) He, R.; Kyu, T. Effect of Plasticization on Ionic Conductivity Enhancement in Relation to Glass Transition Temperature of Crosslinked Polymer Electrolyte Membranes. *Macromolecules* **2016**, *49* (15), 5637−5648.

(32) Huang, L.-Z.; Ma, M.-G.; Ji, X.-X.; Choi, S.-E.; Si, C. Recent Developments and Applications of Hemicellulose from Wheat Straw: A Review. *Front. Bioeng. Biotechnol.* **2021**, *9*, No. 690773, DOI: 10.3389/fbioe.2021.690773.

(33) Schauser, N. S.; Nikolaev, A. F.; Richardson, P. M.; Xie, S.; Johnson, K. A.; Susca, E. M.; Wang, H.; Seshadri, R.; Clément, R. J.; Read, J.; Segalman, R. A. Glass Transition Temperature and Ion Binding Determine Conductivity and Lithium−Ion Transport in Polymer Electrolytes. *ACS Macro Lett.* **2020**, *10* (1), 104−109.
(34) Szcześniak, L.; Rachocki, A.; Tritt-Goc, J. Glass Transition Temperature and Thermal Decomposition of Cellulose Powder. *Cellulose* **2008**, *15* (3), 445−451.
(35) Zelinka, S. L.; Gleber, S.-C.; Vogt, S.; Rodriguez, G. M.; Jakes, J. E. Threshold for Ion Movements in Wood Cell Walls below Fiber Saturation Observed by X-Ray Fluorescence Microscopy (XFM). *Holzforschung* **2014**, *69* (4), 441−448.
(36) Jakes, J. E.; Zelinka, S. L.; Hunt, C. G.; Ciesielski, P.; Frihart, C. R.; Yelle, D.; Passarini, L.; Gleber, S.-C.; Vine, D.; Vogt, S. Measurement of Moisture-Dependent Ion Diffusion Constants in Wood Cell Wall Layers Using Time-Lapse Micro X-Ray Fluorescence Microscopy. *Sci. Rep.* **2020**, *10* (1), No. 9919, DOI: 10.1038/s41598-020-66916-8.
(37) Reyes-Contreras, P.; Mendonça, R. T.; Aguayo, M. G.; Rodríguez, J.; Vega, B.; Fardim, P. Extraction and Characterization of Hemicelluloses from Pinus Radiata and Its Feasibility for Bioethanol Production. *Rev. Arvore* **2013**, *37* (1), 175−180, DOI: 10.1590/S0100-67622013000100018.
(38) Pu, Y.; Zhang, D.; Singh, P. M.; Ragauskas, A. J. The New Forestry Biofuels Sector. *Biofuels, Bioprod. Biorefin.* **2008**, *2* (1), 58−73.
(39) Abraham, M. J.; Murtola, T.; Schulz, R.; Páll, S.; Smith, J. C.; Hess, B.; Lindahl, E. GROMACS: High Performance Molecular Simulations through Multi-Level Parallelism from Laptops to Supercomputers. *SoftwareX* **2015**, *1−2*, 19−25.
(40) Martínez, L.; Andrade, R.; Birgin, E. G.; Martínez, J. M. PACKMOL: A Package for Building Initial Configurations for Molecular Dynamics Simulations. *J. Comput. Chem.* **2009**, *30* (13), 2157−2164.
(41) Huang, J.; MacKerell, A. D. CHARMM36 All-Atom Additive Protein Force Field: Validation Based on Comparison to NMR Data. *J. Comput. Chem.* **2013**, *34* (25), 2135−2145.
(42) Regis, S.; Youssefian, S.; Jassal, M.; Phaneuf, M. D.; Rahbar, N.; Bhowmick, S. Fibronectin Adsorption on Functionalized Electrospun Polycaprolactone Scaffolds: Experimental and Molecular Dynamics Studies. *J. Biomed. Mater. Res., Part A* **2014**, *102* (6), 1697−1706.
(43) Sarkar, D.; Bu, L.; Jakes, J. E.; Zieba, J. K.; Kaufman, I. D.; Crowley, M. F.; Ciesielski, P. N.; Vermaas, J. V. Diffusion in Intact Secondary Cell Wall Models of Plants at Different Equilibrium Moisture Content. *Cell Surf.* **2023**, *9*, No. 100105.
(44) Cousins, W. J. Elastic Modulus of Lignin as Related to Moisture Content. *Wood Sci. Technol.* **1976**, *10* (1), 9−17.
(45) Arzola-Villegas, X.; Lakes, R.; Plaza, N. Z.; Jakes, J. E. Wood Moisture-Induced Swelling at the Cellular Scale—Ab Intra. *Forests* **2019**, *10* (11), 996.
(46) Takamura, N. Studies on Hot Pressing and Drying Process in the Production of Fibreboard III. Softening of Fibre Components in Hot Pressing of Fibre Mat. *J. Jap. Wood Res.* **1968**, *14* (2), 75−79.
(47) Irvine, G. M. The Glass Transitions of Lignin and Hemicellulose and Their Measurement by Differential Thermal Analysis. *Tappi J.* **1984**, *67* (5), 118−121.
(48) Cousins, W. J. Young's Modulus of Hemicellulose as Related to Moisture Content. *Wood Sci. Technol.* **1978**, *12* (3), 161−167.
(49) Olsson, A.-M.; Salmen, L. The Softening Behavior of Hemicelluloses Related to Moisture. In *Hemicelluloses: Science and Technology*; ACS Publications, 2004; pp 184−197.

https://doi.org/10.1021/acs.biomac.3c00857
Biomacromolecules 2024, 25, 666−674

Supplementary Information for Effect of Moisture Content on Ion Diffusion and Glass Transition Temperature in Wood Cell Walls

Sina Youssefian[1,2], Mobin Vandadi[1], Joseph Jakes[3], and Nima Rahbar[1,4*]

The Mean Square Displacements used for the diffusion rate calculation are included in the figures below. For measuring the actual displacement of the ions in the system, the periodic boundaries are unwrapped. The low moisture content systems are stacked on top of each other compared to higher moisture content systems. Thus, the log plot of the data is also included.

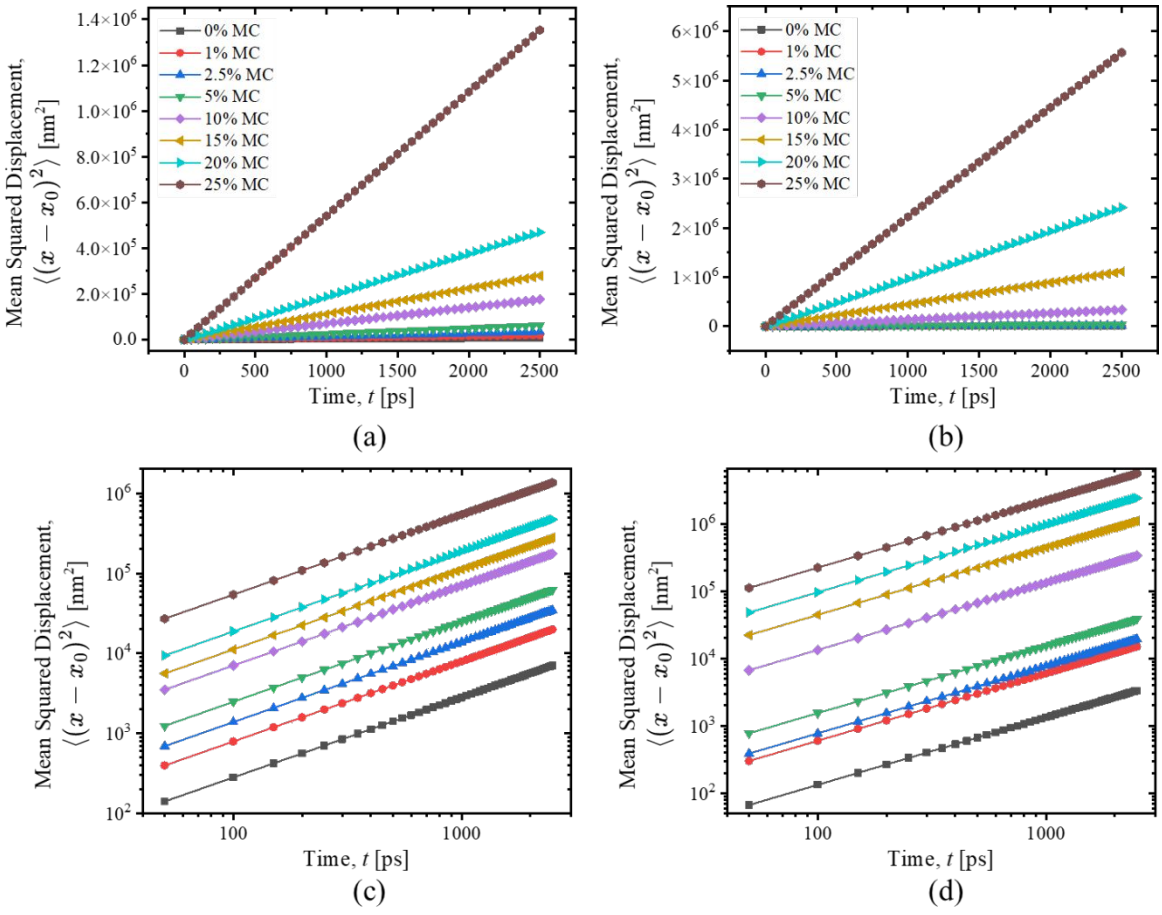

Figure S1: Mean square displacement of the ions diffusion in the 1-ion system for (a,c) potassium ion and (b,d) chloride ion. Since the lines for low diffusion are stacked on top of each other in (a,b), the log-log plot of the MSDs are included in (c,d).